A model for aluminum-dust flames based on particle burning time

A. Gosset[a,b], J. Suarez[a,b], S. Courtiaud[a] and L. Selle[b]
[a]CEA, DAM, Gramat, France
[b]Institut de Mécanique des Fluides de Toulouse, IMFT, Université de Toulouse, CNRS
Toulouse, France

1 Introduction and objectives

Aluminum particles, and more generally metallic particles are of major interest for combustion application because of their high energy density, the possibility to be safely and durably stored and zero carbon emission during oxidation [1]. Therefore, there is a significant body of work on aluminum particles and dust cloud combustion. In early studies [2] it was assumed that aluminum particles burn much like hydrocarbon droplets, i.e. with a diffusion flame surrounding the particle fed by the evaporation of the fuel. Although this description is sometimes correct, the need to account for peculiarities of aluminum combustion has quickly come up [3]. Indeed, metals fuels, due to the high boiling point of their oxides, have combustion products that condense. In the case of aluminum, Al_2O_3 forms a lobe on the particle, interfering with the evaporation of fresh aluminum, thus modifying the combustion properties [4].

The numerical simulation of aluminum combustion is a daunting task, mainly because of the stiff chemical kinetics and the intricacy of phase change. Radiation by the hot aluminum oxide is the icing on the top of this multiphysics, strongly coupled and non-linear problem. A model developed by Brooks and Beckstead [5] showed that the burning time of a particle, which varies proportionally with the square of the diameter for hydrocarbon droplets, is in the case of aluminum a power law, d^n, with n between 1.5 and 1.8. This has then been confirmed by extensive experimental studies [6]. In parallel Catoire *et al.* [7] proposed a scheme that allows the simulation of particles with detailed kinetics. The correlation between the burning time and the particle diameter has then been evaluated [8, 9]. Since then, several experimental studies have confirmed the relation between combustion time and particle diameter [10] allowing the validation of numerical models [11].

Because of the numerical stiffness and computational burden, simpler models for aluminum combustion have been tested for example in the context of segmented solid motors [12, 13]. Although these models allow to compute complex configurations, two main limitations can be pointed out. First, the thermophysical properties of alumina are not taken into account for the residual particle. Second, evaporation still follows a d^2-law, which is usually not adequate for aluminum [10].

In this context, the present work presents a new framework for aluminum-dust combustion, with the intent to reduce the computational burden and numerical stiffness. Because it uses a burning time as the main input, in this study it is referred to as the *integral model*, IM. A comparison with available

Correspondence to: antoine.gosset@imft.fr

experimental data and a more detailed model explicitly resolving chemical kinetics previously developed in the same group [14] (referred to as the *kinetic model*, KM), is presented for the canonical case of a planar flame. The influence of key parameters such as particle diameter, dust concentration and fresh-gases temperature on the flame speed is evaluated. Most results are within experimental uncertainties, which are unfortunately significant for aluminum-dust flames and paths for improvements are proposed when needed. Regarding computational burden, it is shown that the integral model is much faster and more robust than its counterpart using chemical kinetics. This paves the way for a use in more complex cases such as turbulent flames or postcombustion in energetic materials.

2 Model description

The integral model (IM) is developed in a Euler-Lagrange framework. The gaseous phase is described by the compressible Navier-Stokes equations while individual particles are followed along their trajectory, tracking mass, momentum and temperature. The coupling between the two is achieved via source terms for the mass, the momentum and energy.

The cornerstone of the model is the prescription of the combustion time of the particle, given for example by a correlation obtained via experiments. Following [6], a typical correlation reads:

$$\tau_{comb} = \frac{a d_0^n}{X_{eff} P^\alpha T_0^\beta} \tag{1}$$

where a, n, α and β are prescribed coefficients and d_0 the initial diameter of the particle. X_{eff} is the effective oxidizer molar fraction, a weighted sum of oxidising species in the gas phase. In this study, only the reaction with oxygen is considered, therefore $X_{eff} = X_{\mathrm{O}_2}$. With the assumption that during combustion the diameter of the particle d_{Al}^n varies linearly with time [12], one can write:

$$d_{\mathrm{Al}}^n = d_0^n - (d_0^n - d_{res}^n)\frac{t - t_0}{\tau_{comb}} \tag{2}$$

where d_{res}^n is the residual diameter of aluminum. This parameter has been introduced in order to handle cases where combustion is incomplete and is set to 0 in the present work. For a spherical particle, the evaporation mass flow rate $\dot{m}_p$ is linked to the particle diameter via:

$$\dot{m}_p = \frac{d}{dt}(\rho_{\mathrm{Al}} \frac{\pi}{6} d_{\mathrm{Al}}^3) \tag{3}$$

Combining Eqs (2) and (3) yields:

$$\dot{m}_p = -\rho_{\mathrm{Al}} \frac{\pi}{2n} \frac{d_0^n}{\tau_{comb}} d_{\mathrm{Al}}^{3-n} \tag{4}$$

which is the evaporation rate of aluminum, driven by the combustion time τ_{comb}. This relation is similar to the ones described in [12,15]. In order to ensure global mass conservation, the model must account for the consumption of oxidizer in the gaseous phase as well as the condensation of alumina. An additional hypothesis is therefore introduced: the oxidation and condensation are assumed to be complete. This means that all the aluminum evaporated will react in stoichiometric proportions with the oxidizer, and all the alumina produced will condense on the particle. This translates to:

$$\dot{m}_{\mathrm{O}_2,conso} = s\dot{m}_p \tag{5}$$

$$\dot{m}_{\mathrm{Al_2O_3},cond} = -(1+s)\dot{m}_p \tag{6}$$

with $s = {}^{3}/_{4} W_{O_2}/W_{Al}$ the stoichiometric ratio of the global oxidation reaction of aluminum and O_2 and W_k the molar mass of the species k. These equations are driven by the mass flow rate of evaporation, thus by the combustion time according to Eq. (4).

In order to ensure the conservation of energy, the source term in the gaseous phase is written:

$$\Pi_g = \phi_{c,g} - \dot{m}_p(Q_r - Lv_{Al} + (1+s)Lv_{Al_2O_3} - sh_{s,gO_2}) \tag{7}$$

where $\phi_{c,g}$ is the conducto-convective flux, Q_r is the heat of reaction, Lv_k the latent heat of species k and h_{s,gO_2} the sensible enthalpy of O_2. The energy source term, Π_l, in the dispersed phase is then deduced via $\Pi_g + \Pi_l = -\dot{m}_p Q_r$.

For the sake of brevity, the kinetic model (KM) is not presented here. Its essential component is that is uses the kinetic scheme of Catoire *et al.* [7]. The reader is referred to the PhD thesis of Suarez [14] for additional details. Both the IM and KM models have been implemented in the AVBP solver, a 3D compressible LES code developed by CERFACS.

3 Computational setup

The study is conducted on a 1D premixed flame and two meshes are considered: the first one consists of 400 cells with a resolution of $50\,\mu\mathrm{m}$ and the second one is coarser version with 200 cells of $100\,\mu\mathrm{m}$. The parametric space explores variations in particle diameter from $10\,\mu\mathrm{m}$ to $50\,\mu\mathrm{m}$, fresh gases temperature from $300\,\mathrm{K}$ to $600\,\mathrm{K}$ and equivalence ratio from 0.7 to 1. This results in a database of 42 computations. The temporal scheme is a third-order Runge-Kutta scheme and the spatial discretisation uses the approximate Riemann solver HLLC with a MUSCL reconstruction, which is second-order in space.

4 Results and discussion

4.1 Flame structure

First a stoichiometric flame with fresh gases at $300\,\mathrm{K}$ and $15\,\mu\mathrm{m}$ particles is considered. Figure 1 shows the spatial evolution of selected variables across the flame front for the IM (left) and KM (right) computations. As expected, the gas and particle temperature increase across the reaction zone but in the region $3 \leq X \leq 5.5$ for the IM case, there is a visible plateau in the particle temperature and a slight overshoot of the gas temperature. This behaviour stems from the modelling constraint that the particle

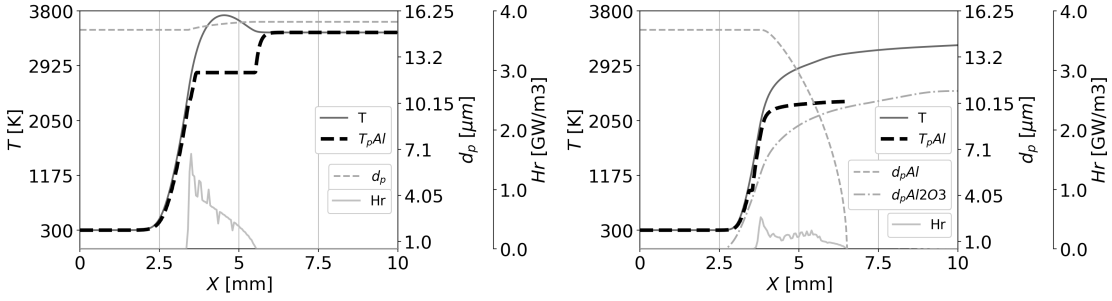

Figure 1: Flame structure: gas temperature, heat-release rate, particle temperature and diameter. Left: integral model (IM). Right: detailed kinetic model (KM).

temperature can not exceed the boiling point of aluminum. The burning rate being fixed via Eq. 4, the gaseous phase takes in the excess heat before the system relaxes to equilibrium. The spatial extent of

this deviation is expected to have a limited pratical impact when using the integral model in practical applications. The evolution is smoother for the KM case but the maximum temperature gradients are comparable in both cases. After the initial surge in temperature, the KM case relaxes slowly, which is a consequence of slower chemical reactions in the gaseous phase. In both models the thickness of the heat-release rate are comparable but its magnitude is larger for the IM. This is a result of the assumption that the combustion is complete and consistent with the slightly higher burnt-gas temperature than in the KM case. Regarding the evolution of the particle diameter, while it monotonously decreases in the KM case, it actually increases in the IM strategy. This stems from the assumption in IM that all the alumina, condenses back on the particle, while in KM it condenses on a separate particle.

4.2 Flame speed

In order to validate these computations, Fig. 2 presents the evolution of flame speed versus diameter (left) and dust concentration (right). First regarding the influence of particle diameter, both the IM and

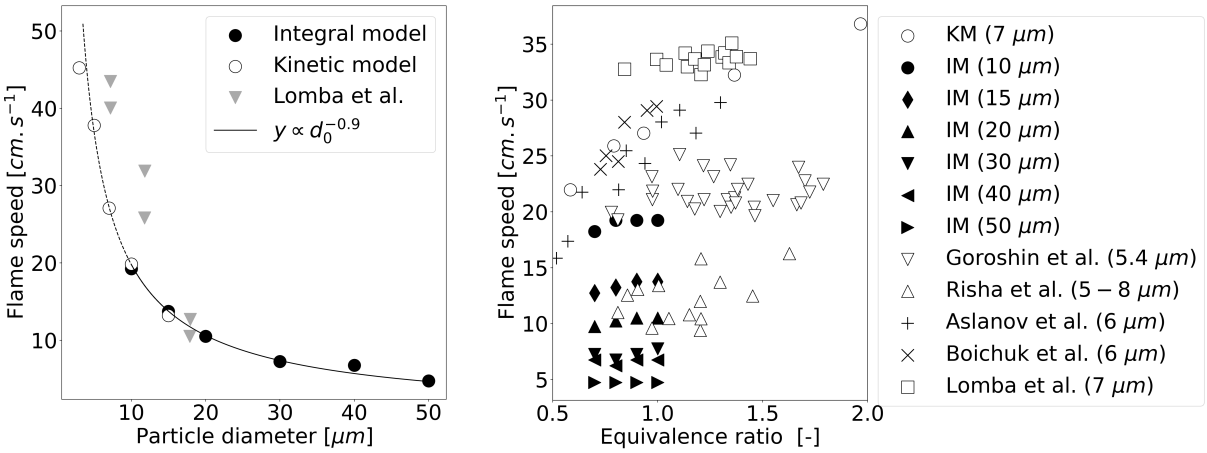

Figure 2: Validation of flame speed for versus experimental data. Left: impact of particle diameter at stoichiometric conditions (experimental data from Lomba et al. [16]). Right: influence of equivalence ratio (Experimental data from burner [17–19] and tube [20, 21] configurations).

KM strategies are consistent and comparable to experimental data, specifically in the range $10\,\mu\mathrm{m}$-$20\,\mu\mathrm{m}$ where they are all available. For smaller diameters, the KM simulations tend to underestimate the flame speed. Nevertheless, the evolution of the flame speeds obtained numerically follows closely the power law $d^{-0.9}$, a trend given by the fact that the laminar flame speed is assumed to be inversely proportional to the square root of the burning time [22], which is itself given by Eq. (1). Figure 2 (right) shows the influence of equivalence ratio. The IM simulations recover the weak sensitivity of aluminum flames to this parameter, which is a great feature for such a simple model. For small diameters, close to the ones used in experimental setup, the IM computations yield flame speeds in between the lowest ($10\,\mathrm{cm\,s^{-1}}$) and highest ($35\,\mathrm{cm\,s^{-1}}$) flame speed measured experimentally. However, the notorious difficulty to control the particle diameter in experiments, coupled with the inherent challenge to stabilize flames with particles of large diameter, makes it tricky to compare more in details the curent IM results with the experimental data available.

4.3 CPU cost

The motivation for the development of the integral model is to reduce the numerical stiffness and computational burden of aluminum combustion simulations. Computational costs for $1\,\mathrm{ms}$ of physical time on

one processor (Intel ® Skylake 6140, $2.3\,\mathrm{GHz}$, 18 cores) are now discussed.Because the kinetic model is so stiff, the maximum value of the CFL for a stable computation is 0.1 (this obviously depends on the numerics), which leads to a CPU cost of $6390\,\mathrm{s}$. For the IM case with the same CFL, the duration of the computation is lowered to $1530\,\mathrm{s}$ but because of its reduced stiffness, the CFL may be increased to 0.5, yielding a further reduction to $310\,\mathrm{s}$. This is more than a twenty-fold acceleration.

4 Conclusions

A new computationally-efficient model for the simulation of aluminum-dust flames, based on a burning time, was presented. The objective is to mitigate the numerical stiffness and computational burden associated with the fast kinetics of aluminum. It has been implemented in the AVBP code and validation cases were presented for 1D flames.

Using available experimental data and a reference model accounting for chemical kinetics, it was shown that the new model predicts quite well the trends of the laminar flame speed when the initial particle diameter or the equivalence ratio are varied. In terms of computational cost, it is up to twenty times faster than its counterpart accounting for chemical kinetics, which paves the way for the simulation of more complex 3D configurations.

References

[1] J. M. Bergthorson, "Recyclable metal fuels for clean and compact zero-carbon power," *Progress in Energy and Combustion Science*, vol. 68, pp. 169–196, 2018.

[2] T. A. Brzustowski and I. Glassman, "Vapor-Phase Diffusion Flames in the Combustion of Magnesium and Aluminum: II. Experimental Observations in Oxygen Atmospheres," *Progress in Astronautics and Rocketry*, vol. 15, pp. 117–158, 1964.

[3] C. K. Law, "A Simplified Theoretical Model for the Vapor-Phase Combustion of Metal Particles," *Combustion Science and Technology*, vol. 7, no. 5, pp. 197–212, 1973.

[4] R. W. Hermsen, "Aluminum Combustion Efficiency in Solid Rocket Motors." *AIAA Paper*, 1981.

[5] K. P. Brooks and M. W. Beckstead, "Dynamics of aluminum combustion," *Journal of Propulsion and Power*, vol. 11, no. 4, pp. 769–780, 1995.

[6] M. W. Beckstead, "Correlating aluminum burning times," *Combustion, Explosion and Shock Waves*, vol. 41, no. 5, pp. 533–546, 2005.

[7] L. Catoire, J.-F. Legendre, and M. Giraud, "Kinetic Model for Aluminum-Sensitized Ram Accelerator Combustion Introduction," vol. 19, no. 2, pp. 196–202, 2003.

[8] E. B. Washburn, J. N. Trivedi, L. Catoire, and M. W. Beckstead, "The simulation of the combustion of micrometer-sized aluminum particles with steam," *Combustion Science and Technology*, vol. 180, no. 8, pp. 1502–1517, 2008.

[9] M. W. Beckstead, Y. Liang, and K. V. Pudduppakkam, "Numerical simulation of single aluminum particle combustion (review)," *Combustion, Explosion and Shock Waves*, vol. 41, no. 6, pp. 622–638, 2005.

[10] A. Braconnier, S. Gallier, F. Halter, and C. Chauveau, "Aluminum combustion in CO2-CO-N2mixtures," *Proceedings of the Combustion Institute*, vol. 38, no. 3, pp. 4355–4363, 2021.

[11] J. Wang, N. Wang, X. Zou, W. Yu, and B. Shi, "Modeling of micro aluminum particle combustion in multiple oxidizers," *Acta Astronautica*, vol. 189, no. July, pp. 119–128, 2021.

[12] A. Sibra, "Modélisation et étude de l'évaporation et de la combustion de gouttes dans les moteurs à propergol solide par une approche eulérienne multi-fluide," Ph.D. dissertation, Université Paris-Saclay, 2015.

[13] L. Lacassagne, "Simulations et analyses de stabilité linéaire du détachement tourbillonnaire d'angle dans les moteurs à propergol solide," Ph.D. dissertation, Institut National Polytechnique de Toulouse, 2017.

[14] J. Suarez, "Modelisation de la combustion diphasique de l'aluminium et application sur la post-combustion d'une charge d'explosif condensé dans l'air," Ph.D. dissertation, Institut national polytechnique de Toulouse, 2020.

[15] J. S. Sabnis, F. J. De Jong, and H. J. Gibeling, "A two-phase restricted equilibrium model for combustion of metalized solid propellants," *AIAA/ASME/SAE/ASEE 28th Joint Propulsion Conference and Exhibit, 1992*, pp. 0–11, 1992.

[16] R. Lomba, S. Bernard, F. Halter, C. Chauveau, C. Mounaïm-Rousselle, P. Gillard, T. Tahtouh, and O. Guézet, "Experimental characterization of combustion regimes for micron-sized aluminum powders," *53rd AIAA Aerospace Sciences Meeting*, no. January, pp. 1–15, 2015.

[17] G. A. Risha, Y. Huang, R. A. Yetter, and V. Yang, "Experimental investigation of aluminum particle dust cloud combustion," *43rd AIAA Aerospace Sciences Meeting and Exhibit - Meeting Papers*, no. January, pp. 8375–8388, 2005.

[18] S. Goroshin, I. Fomenko, and J. H. Lee, "Burning velocities in fuel-rich aluminum dust clouds," *Symposium (International) on Combustion*, vol. 26, no. 2, pp. 1961–1967, 1996.

[19] R. Lomba, P. Laboureur, C. Dumand, C. Chauveau, and F. Halter, "Determination of aluminum-air burning velocities using PIV and Laser sheet tomography," *Proceedings of the Combustion Institute*, vol. 37, no. 3, pp. 3143–3150, 2019.

[20] S. K. Aslanov, V. G. Shevchuk, Y. N. Kostyshin, L. V. Boichuk, and S. V. Goroshin, "Oscillatory combustion of air suspensions," *Combustion, Explosion, and Shock Waves*, vol. 29, no. 2, pp. 163–169, 1993.

[21] L. V. Boichuk, V. G. Shevchuk, and A. I. Shvets, "Flame propagation in two-component aluminum-boron gas suspensions," *Combustion, Explosion and Shock Waves*, vol. 38, no. 6, pp. 651–654, 2002.

[22] H. Cassel, *Some Fundamental Aspects of Dust Flames*. US Department of the Interior,Bureau of Mines, 1964.